Development of Terahertz Focal Plane Array Elements using Sb-based Heterostructure Backward Diodes

Syed Rahman, Yi Xie, Zhenguo Jiang, Huili (Grace) Xing, Patrick Fay and Lei Liu
Department of Electrical Engineering
University of Notre Dame, IN, 46556, USA
Contact: srahman@nd.edu

***Abstract* — We report our initial work on the development of terahertz focal-plane array (FPA) elements by integrating Sb-based heterostructure backward diodes (HBDs) onto folded-dipole antennas (FDAs). Simulation results for a prototype FDA design at 200 GHz have shown that an embedding impedance varying from 10 Ω to 1800 Ω for its real part, and 10 Ω to 900 Ω for the imaginary part can be achieved by changing the antenna geometry for impedance matching. The performance of the 200 GHz FDA on an extended hemispherical silicon lens (R=5 mm) has been analyzed using the ray tracing technique. Optimized antenna directivity and Gaussian coupling efficiency have been obtained with an extension length of 2.5 mm. For a prototype demonstration, an ADS lumped-element nonlinear circuit model has been employed for understanding the HBD device performance at THz frequencies, and on the basis of it, the FDA designed above has been optimized for impedance matching to a HBD device with an active area of 0.4μm×0.4μm at 200 GHz. Under conjugate matching condition, a maximum detector responsivity of ~21,000 V/W could be obtained based on simulation results. Initial work on circuits and devices fabrication is also presented.**

I. Introduction

In recent years, engineers and scientists have intensified their efforts to develop detectors and imaging systems operating in the submillimeter-wave and terahertz (THz) region. The submillimeter-wave and THz range in the electromagnetic spectrum is becoming more and more important to radio astronomy, chemical spectroscopy, bio-sensing, medical imaging, security screening, and defense [1-4]. For all the above applications, a real-time portable THz focal-plane array (FPA) system that can operate at room temperature with high performance has been in high demand for many years [5]. Due to the lack of high performance THz radiation detection devices and other technical challenges, current available THz imaging systems necessitate operation at cryogenic temperature (e.g. HEBs) and/or require slow mechanical scanning [6,7], resulting in bulky and expensive systems. THz detectors employed in room-temperature imagers (e.g. Schottky diodes) generally have relatively low responsivity and high noise equivalent power (NEP) level [8], [9], leading to limited system dynamic range.

Integrated Sb-based heterostructure backward diodes (HBDs) are approaching to meet the demands of high performance FPAs for terahertz imaging systems and applications. Owning to HBDs' high curvature coefficient (i.e. high responsivity), low noise performance, zero bias and room temperature operation, direct detectors based on these devices have been demonstrated at millimeter-wave frequencies [9]. However, reduced HBD device area (e.g. submicron) is required for operation at THz region, resulting in high device impedance. Integrated planar antennas that can potentially achieve high embedding impedances are needed for realizing quasi-optical detector elements with maximized responsivity, which is critical in portable and LNA-less THz FPAs.

In this paper, we report our initial work on the development of FPA elements by integrating Sb-based HBDs onto folded-dipole antennas (FDAs). FDA offers a wide range impedance tuning capacity by varying its geometry such as number of turns, antenna arm width, and arm spacing, thus providing an opportunity to conjugate match the HBD device impedance for maximum responsivity without additional matching network. Ray tracing technique has been applied to calculate the far field radiation patterns of the FDAs mounted on extended hemispherical silicon lens. An optimum extension length of ~2.5 mm has been obtained for maximum directivity and good Gaussian coupling efficiency at 200 GHz [8]. To lessen parasitic effects for THz operation, an airbridge finger has been introduced for integrating HBD devices onto FDAs. For DC signal output, a PBG structure based on co-planar strip lines was designed with low dielectric BCB as the insulation layer. This single element detector design will soon be expanded into a full 2-D FPA for imaging applications.

II. Heterostructure Backward Diodes

Shown in Fig. 1 are the epitaxial layer structure together with energy band diagram of a HBD device. The nonlinear current-voltage (I-V) characteristics of the device are determined by its interband tunneling mechanism between the InAs and GaSb layer. In contrast to Schottky diode the curvature of HBD devices can exceed q/k_BT, resulting in highly sensitive detectors. The unmatched responsivity of HBDs is expressed by,

Manuscript received July 01, 2012. This work is supported by the National Science Foundation (NSF) under contract number of ECCS-1002088 and ECCS-1102214.

S. Rahman, Y. Xie, Z. Jiang, H. Xing, P. Fay and L. Liu are with the Department of Electrical Engineering, University of Notre Dame, IN, 46556, USA.

1000 Å	n+-InAs	$N_D = 1.3x10^{19}$ cm^{-3}
500 Å	n-InAs	$N_D = 1.4x10^{17}$ cm^{-3}
32, 11, 7Å	i-AlSb	
150 Å	i-$Al_{0.1}Ga_{0.9}Sb$	
500 Å	p+-GaSb	$N_A = 1.3x10^{19}$ cm^{-3}
4000 Å	n+-InAs $N_D = 1.3x10^{19}$ cm^{-3}	
S.I. GaAs		

(a)

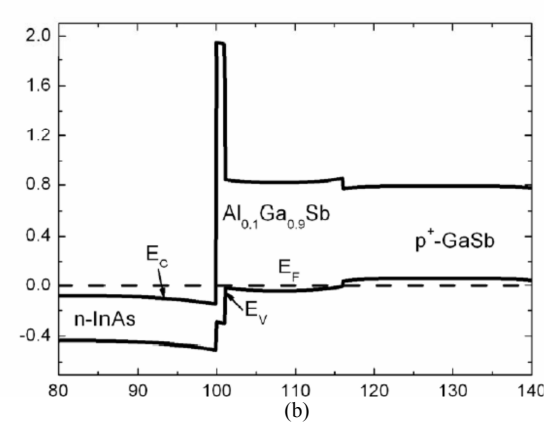

(b)

Fig. 1. (a) Epitaxial layer, and (b) band structure of a Sb-based HBD device.

$$\beta_{v,max} = \frac{\gamma R_j}{2(1+\frac{R_S}{R_j})(1+\frac{R_S}{R_j}+\omega^2 C_j^2 R_S R_j)} \quad (1)$$

where γ, R_j, R_s and C_j are curvature coefficient, junction resistance, series and junction capacitance respectively. A very thin layer of AlSb is grown to provide an additional control over tunneling current density and this additional thin layer increase tunneling probability and reduce junction resistance. However, this layer reduces the device responsivity by lowering the curvature coefficient. The reduced responsivity could be improved by using a p-type δ doping in the cathode layer for reducing junction capacitance and record curvature coefficient has been achieved [9].

The intrinsic cutoff frequency of a HBD device is dependent on its series resistance (R_s) and junction capacitance (C_j) which could be expressed by,

$$f_c = \frac{1}{2\pi R_S C_j}. \quad (2)$$

As the device active area scales down to submicron dimensions, the metal semiconductor contact resistance dominates and the junction capacitance exhibits a fringing capacitance components that does not scale with the active area. Therefore an optimum device area is needed to maximize the cutoff frequency. In addition, the device impedances of

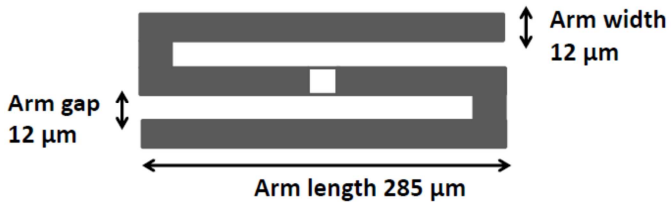

Fig 2: Folded dipole antenna structure with number of turns *N*=3.

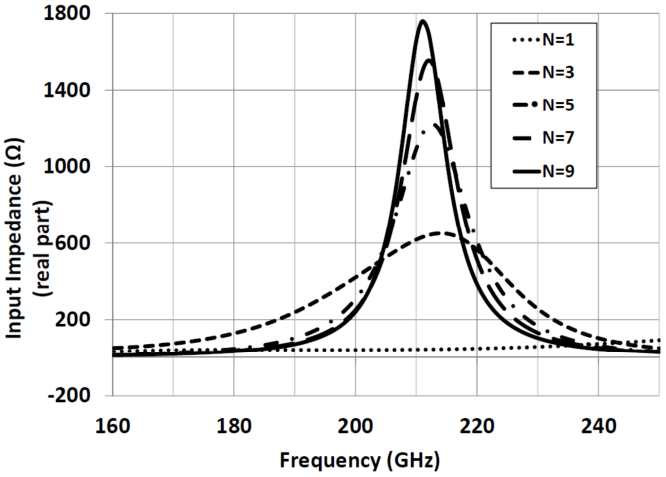

(a)

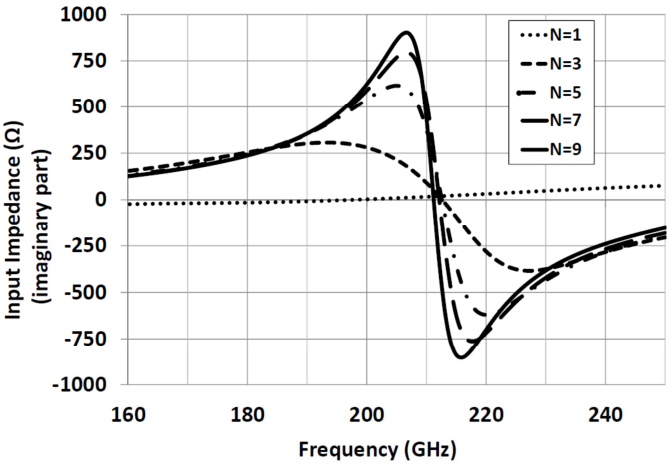

(b)

Fig. 3. Simulation results of a 200 GHz FDA embedding impedance changes with antenna number of turns (*N*): (a) real part antenna embedding impedance, and (b) imaginary part antenna embedding impedance.

HBDs vary with their dimensions and submicron structure HBDs exhibit high impedances at frequencies far below their cutoff frequencies.

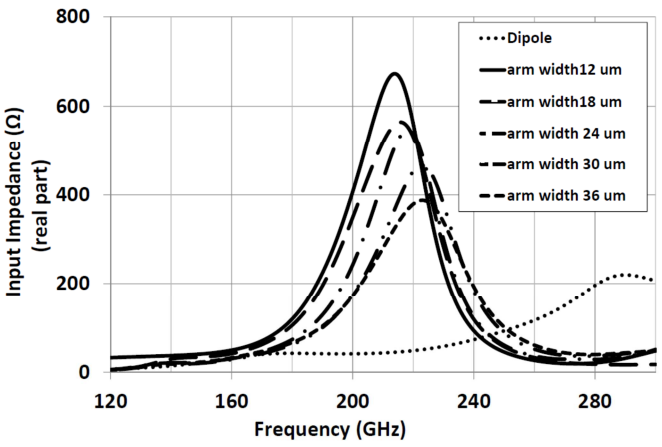

(a)

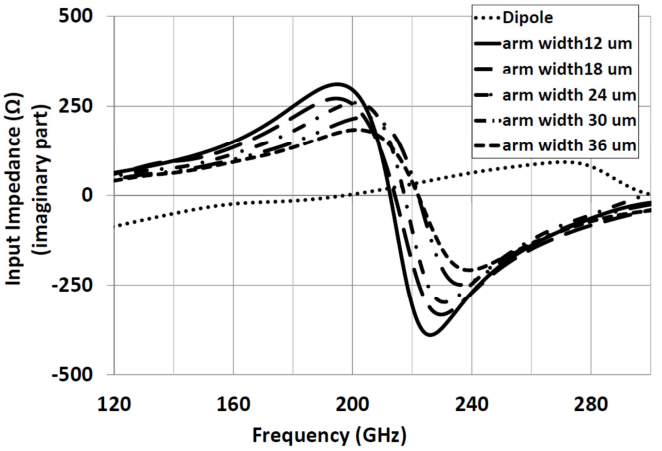

(b)

Fig. 4. Variation of real part (a) and imaginary part (b) of antenna impedance with varying arm width from 12 μm to 36 μm.

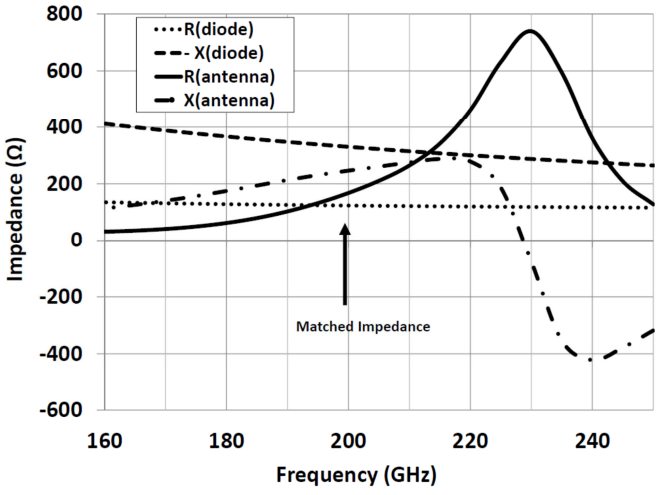

(a)

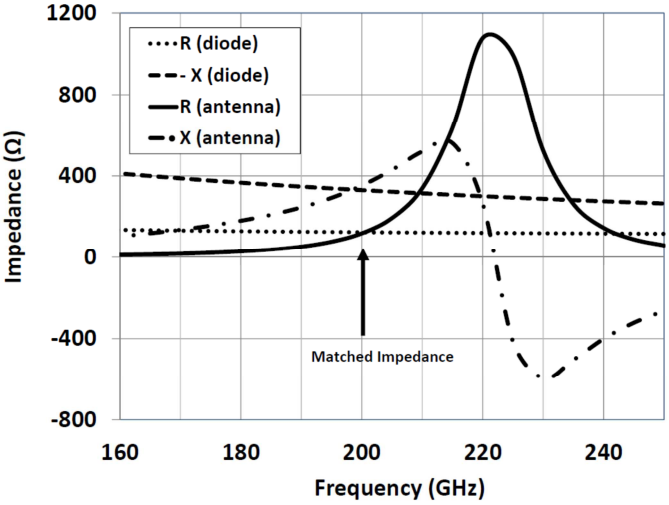

(b)

Fig. 5. FDA designs for impedance conjugate matching to a HBD device (0.4μm×0.4μm) at 200 GH: (a) FDA design with $N=3$, and (b) FDA design with $N=5$.

III. THZ FPA DESIGN AND ANALYSIS

A. Folded Dipole Antennas for Maximum Responsivity

Since submicron scale HBDs exhibit high device impedances at terahertz frequencies, a high impedance antenna with strong tuning capacity is required to achieve maximum responsivity for portable, LNA-less FPAs. Shown in Fig. 2 is a 200 GHz FDA (antenna arm length l = 285) on silicon with number of turns N =3, arm width w=12 μm and arm gap g=12μm. According to antenna theory, the input impedance of a FDA is proportional to N by

$$Z_{in} = N^2 Z_o, \quad (3)$$

where Z_0 is the impedance of a single dipole antenna (N=1) with same antenna arm length and arm width. By varying the antenna geometry such as number of turns, antenna arm width and arm gap, a FDA may provide a wide range of embedding impedances at certain frequency for impedance matching to a HBD device without additional matching network. HFSS simulation has been performed to verify the impedance tuning

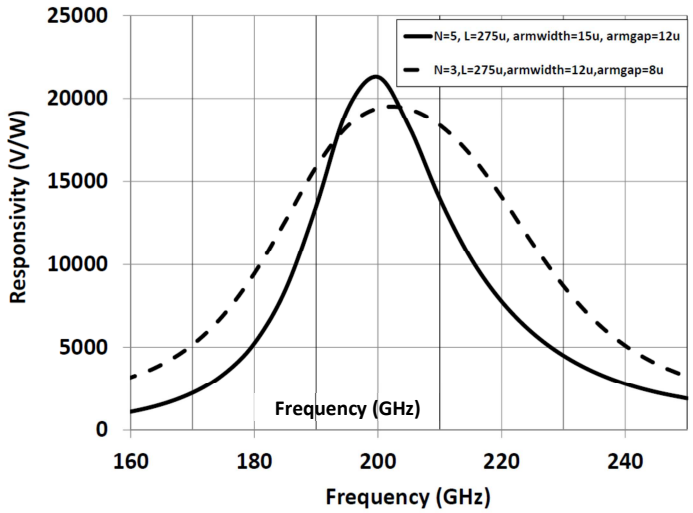

Fig. 6. Simulated detector responsivity under conjugate matching condition at 200 for two antenna designs ($N=3$ and $N=5$).

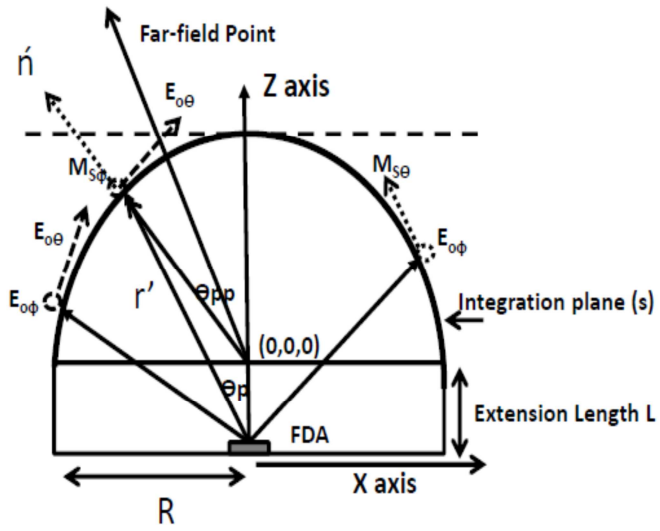

Fig. 7. Ray tracing techniques on extended hemispherical silicon lens.

capability of FDAs as shown in Fig. 3 and Fig. 4. Fig. 3 shows the simulation results for the embedding impedance of a FDA designed with center frequency of ~210 GHz. When the antenna number of turns *N* increases from 1 to 9, the real part of the impedance at 200 GHz changes from 10 Ω to 1800 Ω, while the imaginary impedance varies from 10 Ω to 900 Ω. Fig. 4 illustrates the FDA embedding impedance varies with its arm width *w*. When *w* increase from 12 μm to 36 μm, the antenna real part impedance at 200 GHz changes from 180 Ω to 400 Ω, and the imaginary part impedance varies from 200 Ω to 270 Ω. In addition, HFSS simulation also shows that a FDA impedance can be varied by changing its arm gap from 12 μm to 36 μm (not shown), demonstrating the strong tuning capability of FDAs for impedance matching to achieve a maximum responsivity at certain THz frequency. Two FDAs have been designed for impedance matching to a HBD device with an active area of 0.4μm×0.4μm at 200 GHz. On the basis of a lumped element circuit model, the HBD device

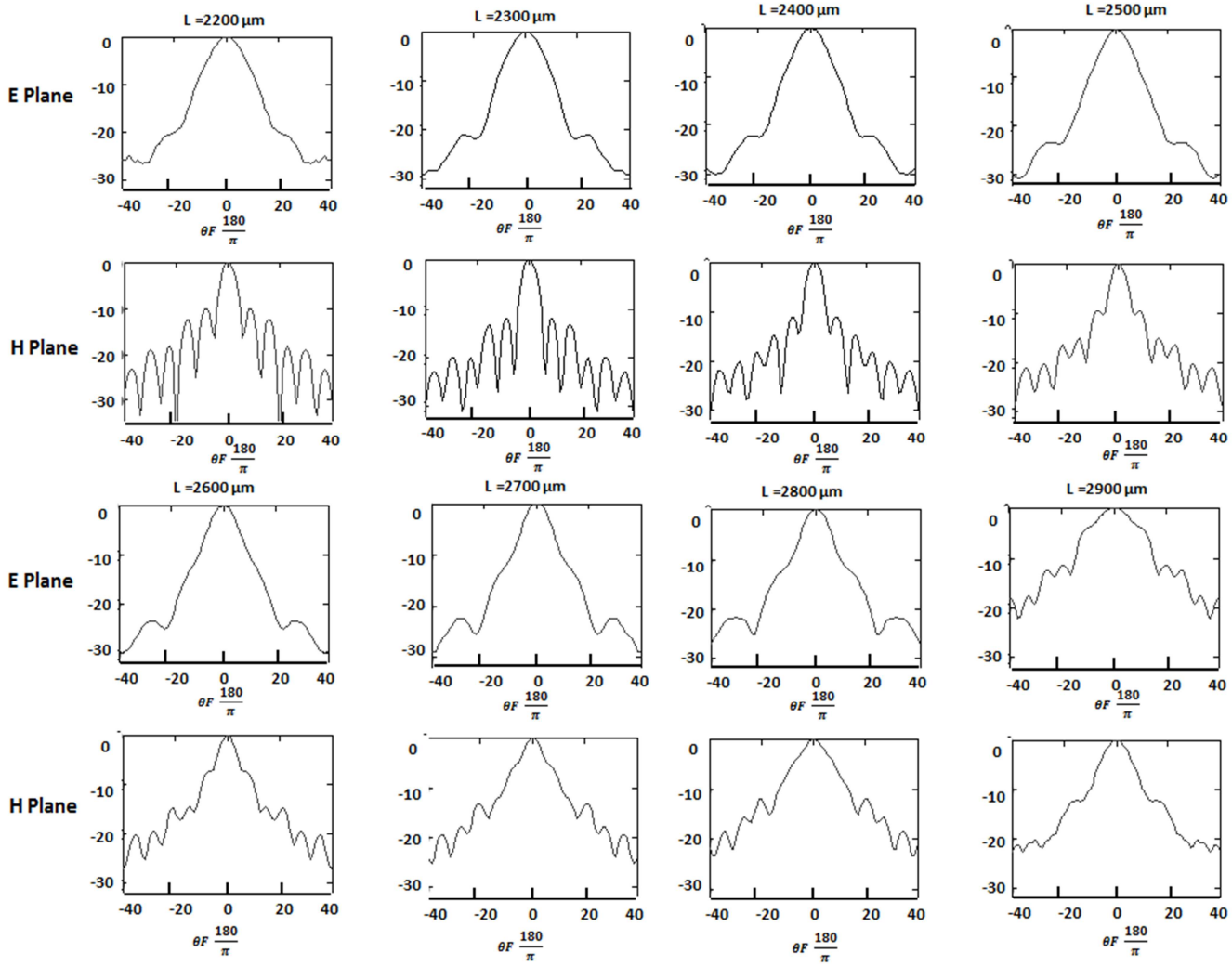

Fig. 8. E and H plane radiation patterns of FDA with N=3 at 200 GHz calculated for extension lengths varying from 2200 μm to 2900 μm.

antenna arm length of 275 μm, an arm width of 15 μm and an arm gap of 12 μm. The second design uses the antenna parameters of *N=5, l= 275* μm,*w=12* μm, and *g = 10* μm. As shown in Fig. 5 (a) and (b), nearly perfect conjugate impedance matching has been achieved for both antenna designs. Under this impedance matching conditions, the detector responsivities have been calculated as shown in Fig. 6. Maximum responsivities of 19500 V/W and 20000 V/W have been demonstrated for *N*=3, and *N*=5 antennas respectively. Because FDAs are resonant antennas with reduced bandwidth for increased number of turns, the detector element with *N*=5 design shows relatively narrower bandwidth as compared to the design with *N*=3.

B. Lens-Coupled FDA Far-Field Radiation Patterns

To calculate far field radiation pattern of the folded dipole antennas mounted on an extended hemispherical silicon lens with radius R = 5 mm, ray tracing technique has been applied [8] to choose an extension length for highest antenna directivity while keeping an acceptable Gaussian coupling efficiency, as shown in Fig. 7.

Fig. 8 shows the simulation results of far-field radiation patterns of the lens-coupled *N*=3 FDA at 200 GHz. For an extension length varies from 2200 μm to 2900 μm the far-field patterns in both the E-plane and H-plane become narrower first and then broader with a highest directivity achieved for 2.5 mm extension length.

C. Low Pass Filter Design

A co-planar strip-line stepped-impedance low-pass filter has been designed to extract DC signal, while presenting open-circuit to the designed FDA [12]. The length of each section is 135 μm. For the high impedance sections, the strip line width (*h*) is 2 μm and the gap between the lines (*t*) is 82 μm, while for the low impedance sections, *h*= 41 μm and t = 4 μm. Fig. 9 shows the simulated s-parameters and the obtained RF suppression at around 200 GHz is as high as 32 dB.

IV. Integrated HBD Detector Fabrication

The fabrication of the designed HBD FPA detector element has been performed at the nanofabrication facility of the University of Notre Dame. Fig. 10 shows the process flow including 1) epitaxial layer growth (see Fig. 1) on semi-insulation GaAs wafer, 2) HBD device active area definition and mesa etching, 3) antenna layer photolithography, 4) airbridge formation, and 5) BCB layer insulation and LPF layer photolithography. The active area of HBD devices was defined by top contact cathode layer of Ti/Au/Ti (20 nm/250 nm/ Au). This layer also serves as the mask layer in the subsequent self-aligned wet chemical etching of the active device junction fabrication. The bottom Ti layer increase adhesion of the cathode contact and the top Ti layer minimize the electro chemical effects in the sub-sequent chemical etching since electro chemical effect degrade the process and degrade lateral scaling of the device.

Two types of etchants: citric acid+H_2O_2 (1:2) and NH_4OH+H_2O (1:5) have been used to etch the InAs and Sb bearing materials, respectively. Following the active area etching the device was isolated by wet etching of InAs anode contact to define the mesa anode layer. The FDA antenna layer was then fabricated using a photolithography and lift-off process.

To minimize parasitic effects, an airbridge finger has been introduced across the antenna and device cathode contact as shown in fig 9. Polyimide material was utilized as the sacrificial layer for airbridge development. The polyimide sacrificial layer was spanned, partially cured and etched down using RIE. After exposing the antenna layer and cathode contact, a very thin Ti layer (15 nm) was deposited to protect the polyimide layer from the subsequent airbridge fabrication process. The airbridge finger was then fabricated using conventional photolithography followed by lift-off process.

A layer of BCB was spanned, hard cured and patterned by RIE to serve as the isolation material between the antenna layer and LPF circuits. The polyimide sacrificial layer was removed by isotropic dry etching before developing the DC output/LPF circuits (1 μm). Fig. 11 shows a SEM picture of a HBD device with an airbridge finger integrated at the center of a FDA. The fabricated HBD detector elements will soon be tested and expanded into a full 2-D FPAs.

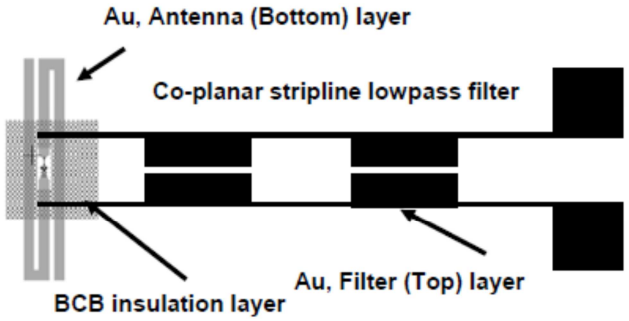

(a)

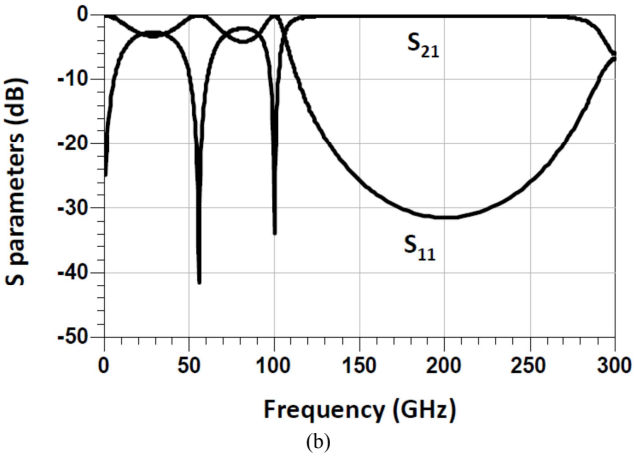

(b)

Fig. 9. Low pass filter design to suppress 200 GHz signal (a) and simulated S_{11} and S_{21} parameters (b).

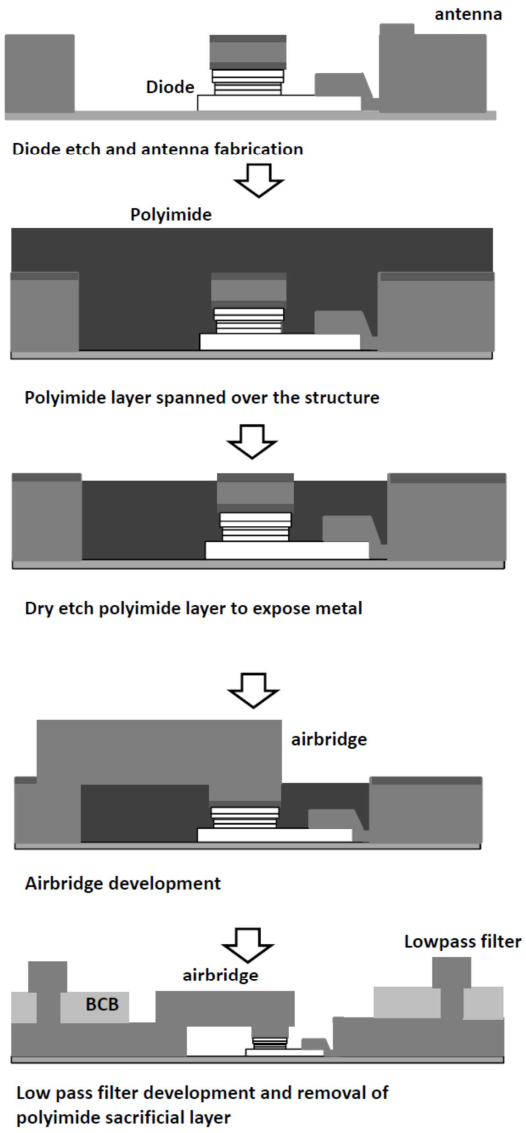

Fig. 10. Process flow diagram for the development of integrated HBD detector.

V. Conclusion

High performance THz detector elements for focal-plane imaging array applications have been designed, simulated and fabricated based on heterostructure backward tunneling diodes. For conjugate impedance matching to achieve maximum detector responsivity, FDAs with strong tuning capability have been simulated and designed. A detector responsivity of ~ 20000 V/W can be potentially achieved at 200 GHz using FDAs without additional impedance matching network, making the element design suitable for portable, LNA-less THz FPAs. Ray tracing technique has been applied to calculate the far field radiation patterns of the FDAs mounted on extended hemispherical silicon lens. An optimum extension length of ~2.5 mm has been obtained for maximum directivity and good Gaussian coupling efficiency at 200 GHz. To lessen parasitic effects of HBDs for THz operation, an airbridge finger has been introduced for integrating HBD devices onto FDAs. For DC signal output, a PBG structure based on co-planar strip lines was designed with low dielectric BCB as the insulation layer. This single element detector design will soon be expanded into a full 2-D FPA for imaging applications.

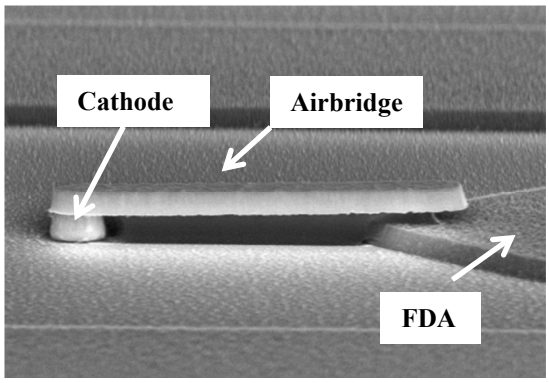

Fig. 11. The integrated HBD device at the center of a FDA with airbridge structure for reducing parasitic effects.

Acknowledgement

This work is supported by the National Science Foundation (NSF) under contract number of ECCS-1002088 and ECCS-1102214. The authors would like to thank people of the Notre Dame Nanofabrication (NDNF) facility for discussion and assistance. The authors also thank the support from the Advanced Diagnostics and Therapeutics Initiative (AD&T) at the University of Notre Dame.

References

[1] P.H. Siegel, "THz Technology" *IEEE Trans. Microwave Theory Tech.,* vol. 50, no. 3, pp. 910-928, March 2002.

[2] D.B. Rutledge and M.S. Muha, "Imaging antenna arrays," *IEEE Trans. Antennas and Propagat.*, vol. AP-30, no. 4, pp. 535–540, July 1982.

[3] P.H. Siegel, "THz Technology in Biology and Medicine*," IEEE Trans. Microwave Theory Tech.*, vol. 52, no. 10, pp. 2438-2448, Oct. 2004

[4] L. Liu, J. L. Hesler, H. Xu, A. W. Lichtenberger, and R. M. Weikle, "A broadband quasi-optical terahertz detector utilizing a zero bias Schottky diode," *IEEE Microw. Wireless Compon. Lett.*, vol. 20, no. 9, pp. 504–506, Sep. 2010.

[5] S. Cherednichenko, A.Hammar, S. Bevilacqua, V. Drakinskiy, J. Stake, and A. Kalabukhov, "A Room Temperature Bolometer for Terahertz Coherent and Incoherent Detection", *IEEE Trans..on Terahertz Science Tech.,* Vol. 1, No. 2, pp. 395-402, Nov 2011

[6] Z. Zhang,"Sb-Heterojunction backward diodes for direct detection and passive millimeter-wave imaging", *PhD thesis,* University of Notre Dame, 2011.

[7] N. Su, R. Rajavel, P. Deelman, J. N. Schulman, and P. Fay, "Sb-Heterostructure millimeter-wave detectors with reduced capacitance and noise equivalent power," *IEEE Electron Device Lett.*, vol. 29, no. 6, pp. 536–539, Jun. 2008.

[8] D. F. Filipovic, S. S. Gearhart, and G. M. Rebeiz, "Double-slot antennas on extended hemispherical and elliptical silicon dielectric lenses*," IEEE Trans. Microwave Theory Tech.*, vol. 41, no. 10, pp. 1738-1749 Oct. 1993.

[9] Z. Zhang, R. Rajavel, P. Deelman, and P. Fay, "Sub-Micron Area Heterojunction Backward Diode Millimeter-Wave Detectors With 0.18 pW/Hz$^{1/2}$ Noise Equivalent Power", *IEEE Microw. Wireless Compon. Lett.*, vol. 21, no. 5, 2011.

[10] H. C. Ryu, S. I. Kim, M. H. Kwak, K. Y. Kang, and S. O. Park, "Afolded dipole antenna having extremely high input impedance for continuous-wave terahertz power enhancement," *33rd Int.Conf.*

Infrared, Millimeter, and Terahertz Waves (IRMMW), Pasadena, California, USA, Sep. 2008.

[11] C.A. Balanis, "Antenna Theory", Third Edition, 2005

[12] L. Liu, H. Xu, Y. Duan, A. W. Lichtenberger, J. L. Hesler, and R. M. Weikle, II,"A 200 GHz Schottky Diode Quasi-Optical Detector Based on Folded Dipole Antenna", *ISSTT 2009,* Charlottesville, VA, USA.